

## Logarithmic decay laws in glassy systems

This article has been downloaded from IOPscience. Please scroll down to see the full text article.

1989 J. Phys.: Condens. Matter 1 4203

(<http://iopscience.iop.org/0953-8984/1/26/015>)

View [the table of contents for this issue](#), or go to the [journal homepage](#) for more

Download details:

IP Address: 171.66.16.93

The article was downloaded on 10/05/2010 at 18:23

Please note that [terms and conditions apply](#).

## Logarithmic decay laws in glassy systems

W Götze† and L Sjögren

Institute of Theoretical Physics, Chalmers University of Technology, S-412 96 Göteborg, Sweden

Received 17 November 1988, in final form 1 February 1989

**Abstract.** The equations for the  $\beta$  relaxation dynamics as obtained within mode-coupling theory for the glass transition are solved asymptotically for parameters near Whitney cusp singularities. The solution is given by a two-parameter scaling law, where the time  $t$  enters as  $\ln t$  and where the scaling times depend exponentially with a Vogel–Fulcher like form on the control parameters. The master function is given in terms of Weierstrass' elliptic function. It describes crossovers from critical relaxation  $\Phi(t) \propto 1/\ln^2 t$  to a constant  $f_0$ , to a power-law decay  $1/t^a$ , to  $\Phi(t) \propto -\ln t$ , or to  $\Phi(t) \propto \ln^2 t$  depending on the sector in parameter space. The relaxation data for the Cu–Mn spin-glass alloy can be described by the theory for a time interval of eight decades.

### 1. Introduction

The glass transition singularities, which appear in mode-coupling theories, can be classified according to underlying topological singularities of certain mappings in high-dimensional spaces. The dynamics of the  $\beta$  relaxation region is specified by a few relevant parameters whose number is characteristic for every type of singularity. The simplest singularities are  $A_2$  cusps or Whitney folds. In this case power-law relaxation is found at the critical point and scaling laws describe the dynamics near the transition. If the system exhibits a certain asymmetry, as expected e.g. between charge and mass fluctuations in ionic melts, a  $\beta$  peak may occur. It is located above the known  $\alpha$  resonance and it exhibits stretching over many decades. In the strong-coupling limit the shape function is given by a Cole–Cole formula. These and other findings indicate that the singularities connected with Whitney folds are relevant for a description of structural glass transitions as observed in simple glass-forming undercooled liquids (see Götze and Sjögren 1989 and references therein).

For spin-glass transitions neutron scattering discovered relaxation stretching (Mezei and Murani 1979) even larger than that detected recently for structural glass transitions (Mezei *et al* 1987, Richter *et al* 1988). But while the latter data obey a scaling law, the time–temperature superposition principle, the former do not show such simplicity. A major part of the spin-glass data can be described by a  $c \ln t$  law, where the prefactor  $c$  depends sensitively on temperature (Mezei and Murani 1979, Binder and Young 1986). Such logarithmic decay is not known for structural glass transitions. It was noticed (Götze and Haussmann 1988) that the mentioned spin-glass results are generic features

† On sabbatical leave from: Physik-Department der Technischen Universität München, D-8046 Garching, and Max-Planck-Institut für Physik und Astrophysik, D-8000 München, Federal Republic of Germany.

of the  $A_3$  glass transition singularity, the next more complicated scenario connected with Whitney cusps. Such a singularity is exhibited in a mode-coupling theory for a conventional microscopic spin-glass model, which was formulated some years ago. In particular a simple one-component model for the spin-glass transition was examined (Götze and Sjögren 1984); its numerical solution can account semi-quantitatively for the two decades of relaxation dynamics covered by the mentioned neutron scattering work (Götze and Haussmann 1988). Therefore we want to pursue this line and study the complete  $\beta$  relaxation for this Whitney cusp singularity.

The paper is organised as follows. After a compilation of the necessary dynamic equations for the  $\beta$  relaxation we derive the  $\Phi(t) \propto 1/\ln^2(t/t_1)$  law for the critical decay at the cusp singularity for the correlator  $\Phi$  as a function of time  $t$ . The leading correction to this asymptotic law is also determined. Then the crossover between the critical logarithmic decay and the normal power-law decay is described by a logarithmic scaling law. This concept denotes a conventional dynamic scaling law, where however the normal time  $t$  is replaced with  $\ln(t/t_1)$ . In § 4 it will be shown that there are only two relevant parameters ( $\xi, \eta$ ) for the description of the dynamics near a Whitney cusp. Connected with these parameters there are two characteristic timescales ( $t_\xi, t_\eta$ ) which diverge for  $\xi \rightarrow 0$  or  $\eta \rightarrow 0$  respectively, where  $(\xi, \eta) = (0, 0)$  specifies the cusp. The divergence of the scales is the reason for the slowing down of the motion near an  $A_3$  singularity. The dynamics is described by a two-parameter logarithmic scaling law, where the two relevant parameters are  $\ln(t_\xi/t_1)$  and  $\ln(t_\eta/t_1)$  respectively. The master function is given in terms of Weierstrass' elliptic function. There are two hypersurfaces  $\xi = 0$  and  $\eta = 0$  where the general result specialises to simple one-parameter logarithmic scaling laws. They describe the crossover from the critical decay to a  $\ln(t/t'_\xi)$  or a  $\ln^2(t/t'_\eta)$  relaxation law respectively. In the conclusions some possibilities for generalisations or applications of our theory are discussed.

## 2. Dynamic equations

The general equations for the  $\beta$  relaxation have been derived in a preceding paper to be referred to as GS (Götze and Sjögren 1989). To keep the following calculations self-contained from a mathematical point of view we will collect the most relevant starting equations from GS in this section. Our results will be exemplified by solutions for a dynamic model dealing with one correlation function  $\Phi(z)$ , which obeys

$$\Phi(z) = -1/\{z - 1/[(z + i\nu)/\Omega^2 + \text{LT}[F(\Phi(t))](z)]\}. \quad (2.1)$$

Correlator  $\Phi(z)$  is a positive analytic function of complex frequency  $z$ . It is the Laplace transform of a real even correlation function  $\Phi(t)$  of time  $t$ , and is defined as in GS equation (1.1). Parameter  $\Omega > 0$  is the characteristic microscopic frequency scale and  $\nu \geq 0$  is a stochastic friction constant. The mode-coupling functional  $F$  is a polynomial with coefficients  $v_n \geq 0$  given in GS equation (1.4b). The  $v_n$  are the mathematical control parameters of the theory; they are combined to a vector  $V$  in control parameter space  $\mathbf{R}_N$ . We will show results for the  $F_{12}$  model, specified by  $F(f) = v_1 f + v_2 f^2$ , and for the  $F_{13}$  model, specified by  $F(f) = v_1 f + v_3 f^3$ . The latter form is relevant for spin-glass transitions and the former for structural glass transitions.

Near glass transitions a microscopic time  $t_m$  and a corresponding frequency  $\Omega_m = 2\pi/t_m$  are defined implicitly so that the regular term  $(z + i\nu)/\Omega^2$  in (2.1) is much smaller compared with the mode-coupling term for  $|z| \ll \Omega_m$ ,  $t \gg t_m$ . Then one can drop the

$(z + i\nu)$  term in equation (2.1). The resulting equation, which describes  $\alpha$  as well as  $\beta$  relaxation, is scale-invariant; with  $\Phi(t)$  also  $\Phi^y(t) = \Phi(t/y)$  is a solution for all  $y > 0$ . Hence the scale for the dynamics cannot be fixed by the following analysis. It is determined by matching of the solutions via variations of  $y$  to the correct short-time solution of equation (2.1) for  $t \sim t_m$ . Let us introduce a real parameter  $\tilde{f}$  in order to write

$$\Phi(t) = \tilde{f} + G(t) \quad z\Phi(z) = -\tilde{f} + zG(z). \tag{2.2}$$

Parameter  $\tilde{f}$  will be specified later, so that some simplifications occur in the equations of motion. The real problem is the determination of  $G(t)$ . The  $\beta$  regime will be studied and this was characterised in GS implicitly by two inequalities:

$$|zG(z)/(1 - \tilde{f})| \ll 1 \tag{2.3a}$$

$$|\text{LT}[G^{n+1}(t)](z)/\text{LT}[G^n(t)](z)| \ll 1. \tag{2.3b}$$

In this regime the dynamic equations read:

$$\begin{aligned} &(-\delta_0/z) + \delta_1 G(z) \\ &+ (1 + \delta_2)\text{LT}[G^2(t)](z) + zG^2(z) \\ &+ (\gamma_3 + \delta_3)\text{LT}[G^3(t)](z) - \gamma_3 z^2 G^3(z) \\ &+ (\gamma_4 + \delta_4)\text{LT}[G^4(t)](z) + \dots = 0. \end{aligned} \tag{2.4}$$

The coefficients  $\gamma_k$  and  $\delta_k$  depend on  $\tilde{f}$  and  $V$ :

$$\delta_k = (\partial^k \Delta F / \partial \tilde{f}^k)(1 - \tilde{f}^3/k!) \tag{2.5a}$$

$$\Delta F = F - \tilde{f}(1 - \tilde{f})^{-1} \tag{2.5b}$$

$$\gamma_k = 1/(1 - \tilde{f})^{k-2}. \tag{2.5c}$$

The non-ergodicity parameter of the theory, the glass form factor  $f = \Phi(t \rightarrow \infty)$ , is obtained from  $\Delta F(V, f) = 0$ , where the variables have been indicated for the sake of clarity. Glassy states are those  $V$  where the solution yields  $f > 0$ . Glass transition singularities are the bifurcation singularities  $(V_c, f_c)$ . The relevant singularities are cuspsoids  $A_l$  of degree  $l = 2, 3, \dots$ . Denoting  $\delta_k^c = \delta_k(V_c, f_c)$ , cuspid  $A_l$  is characterised by  $\delta_k^c = 0, k \leq l - 1, \delta_l^c \neq 0$  (Arnold 1986). Since the  $\delta_k$  are also the relevant parameters entering the full dynamic equation (2.4), the various glass transition singularities can be classified according to the cuspid degree. The simplest singularity is the Whitney fold  $A_2$ . The set  $S_c$  of fold singularities is a hypersurface in  $R_N$ . The dynamics was discussed in detail in GS. In this paper the next type of singularities, the Whitney cusps  $A_3$ , will be analysed. The corresponding points  $V_c$  are endpoints of  $S_c$ . They will be referred to as simple endpoints, in order to distinguish them from the complicated ones  $A_l, l > 3$ . If one introduces the exponent parameter  $\lambda = 1 + \delta_2^c$  and the cusp parameter  $\mu = -\delta_3^c$ , the simple endpoints are characterised by  $\lambda = 1, \mu > 0$ . Explicit expressions for  $\lambda, \mu$  are given in equations (3.1) of GS. The  $F_{12}$  model has one endpoint, where

$$v_1^c = 1 \quad v_2^c = 1 \quad f_c = 0 \quad \mu = 1 \quad F_{12} \text{ model.} \tag{2.6a}$$

The  $F_{13}$  model also has one endpoint with

$$v_1^c = \frac{9}{8} \quad v_3^c = \frac{27}{8} \quad f_c = \frac{1}{8} \quad \mu = 1 \quad F_{13} \text{ model.} \tag{2.6b}$$

Equation (2.4) is the basic starting point for our analysis of the relaxation behaviour at  $A_2$  and  $A_3$  singularities, as well as higher-order ones. However with every cuspid  $A_k$  there is a distinct new topological scenario as compared with previous ones of lower order. So the solution for the present case  $\delta_2 = 0$  but  $\delta_3 \neq 0$ , characterising the cusp  $A_3$ , is not a special case or simple limit of the solution for the fold  $A_2$ , with  $\delta_2 < 0$ , analysed in GS.

### 3. Critical decay

Let us consider first the solution of the dynamic equations for parameters  $V_c$  at the endpoint. The solution will be referred to as critical relaxation. In this case we choose  $\hat{f} = f_c$  so that  $\delta_0 = \delta_1 = \delta_2 = 0$ ; then equation (2.4) specialises to

$$\begin{aligned} & \text{LT}[G^2(t)](z) + zG^2(z) \\ & - \mu \text{LT}[G^3(t)](z) \\ & + \gamma_3^2 \{ \text{LT}[G^3(t)](z) - z^2 G^3(z) \} + \delta_4^2 \text{LT}[G^4(t)](z) + \dots = 0. \end{aligned} \tag{3.1}$$

To solve this equation we exploit the property

$$L(i/z) \sim -z \text{LT}[L(t)](z) \tag{3.2}$$

an asymptotic equality for  $z \rightarrow 0$ , which follows from the Tauberian theorem for so-called slowly varying functions  $L(t)$ . The latter are defined by the property  $L(tx)/L(t) \rightarrow 1$  for  $t \rightarrow \infty$  for all  $x > 0$  (Feller 1971, ch. 13). Therefore every  $G(t) = L(t)$  will make the first line of equation (3.1) vanish in leading order, since with  $L$  also  $L^2$  is a slowly varying function. If one now chooses  $L$  properly, one can use the corrections to the leading contributions of the first line in equation (3.1) to cancel the leading contribution of the second line, etc. Examples for slowly varying functions are powers of logarithms,  $\ln^k t$ , or iterations of logarithms like  $\ln \ln t$  or combinations thereof. This suggests as a first step to represent the correlator  $G$  in terms of another function  $g$  by the definition

$$G(t) = g[\ln(t/t_1)]. \tag{3.3}$$

One then expects  $g$  to be simpler than  $G$  itself. The question of choosing  $g$  properly in order to achieve the mentioned cancellations is then equivalent to a solution of an ordinary differential equation, as is shown in the Appendix. From equation (A.13) one obtains the leading-order critical correlator

$$G_0(t) = \rho^2 / \ln^2(t/t_1) \tag{3.4a}$$

$$G_0(z) = \rho^2 (-1/z) / \ln^2(-izt_1). \tag{3.4b}$$

Inclusion of the next-to-leading-order term yields

$$G(t) = G_0(t)[1 + C(t) + \dots] \tag{3.5a}$$

where

$$C(t) = [6\zeta(3)/\zeta(2)] \ln \ln(t/t_1) / \ln(t/t_1). \tag{3.5b}$$

Here  $\rho^2 = 4\zeta(2)/\mu$  and  $\zeta(2) = \pi^2/6 \approx 1.645$ ,  $\zeta(3) \approx 1.202$  denote Riemann's  $\zeta$ -function. For  $t \rightarrow \infty$  the correction  $C$  can be neglected,  $G(z)$  is positive analytic and inequalit-

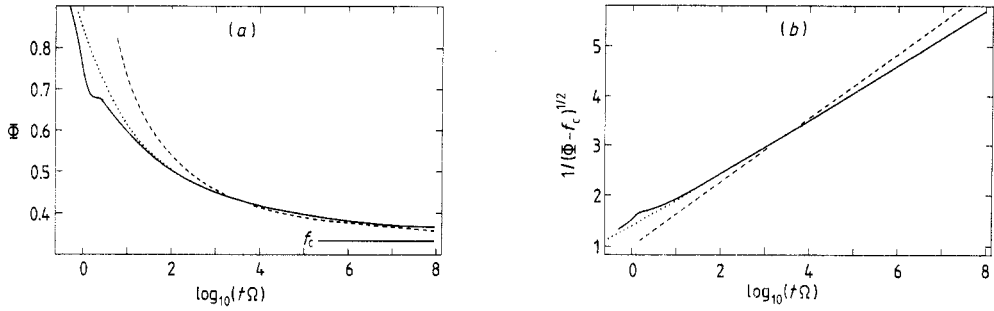


**Figure 1.** (a) Plot of  $\Phi(t)$  versus  $\log_{10}(t\Omega)$ . Full curve represents the  $F_{13}$  model with  $\nu_1 = \frac{8}{9}$ ,  $\nu_3 = \frac{27}{8}$  and  $\nu = \Omega$ . Broken curve shows  $\frac{1}{3} + G_0(t)$  with  $G_0(t)$  given in equation (3.4a) with  $\log_{10}(t_1\Omega) = -1.50$ , and dotted curve shows  $\frac{1}{3} + G(t)$  with  $G(t)$  given in equation (3.5a), with  $\log_{10}(t_1\Omega) = -3.25$ . (b) Plot of  $[\Phi(t) - \frac{1}{3}]^{-1/2}$  versus  $t\Omega$  for the same data as in (a).

ies (2.3) are obeyed. Hence equations (3.4) provide an asymptotic solution for the original equation (2.1).

There is some critical time  $t_1^c$  such that  $G(t)$  exceeds unity for  $t < t_1^c$ . Similarly,  $\Phi(z)$  is not positive analytic any more if  $|z| > 1/t_1^c$ . Hence the leading-order solution found can be used only for  $t > t_1^c$ , where

$$t_1^c = t_1 e^\rho. \tag{3.6}$$

Since we restrict the discussion to simple endpoints,  $\mu$  is of order unity. Hence  $t_1$  can be chosen such that  $t_1^c$  is of order  $t_m$  and such that matching of the asymptotic solution to the microscopic one is achieved. As a result, equation (3.5) describes the dynamics for all times outside the microscopic region. This conclusion will be exemplified by two diagrams. In figure 1(a) the full curve reproduces  $\Phi(t)$  from numerical solution of the  $F_{13}$  model (Götze and Haussmann 1988). The dotted curve is the result (3.5) with  $t_1$  adjusted to  $\log_{10}(t_1\Omega) = -3.25$ . The correction term  $C(t)$  varies between 1.06 and 0.65 if  $t$  increases over six decades. Therefore the leading asymptote  $G_0$ , shown as the broken curve with the choice  $\log_{10}(t_1\Omega) = -1.50$ , is not an adequate description of the data for the time interval considered. In figure 1(b) the full curve represents  $[\Phi(t) - \frac{1}{3}]^{-1/2}$  for the same data as in figure 1(a). The dotted and broken curves show the same quantity for the analytic results (3.5) and (3.4a) respectively. In this plot the leading asymptote  $G_0$  yields a straight line with a slope given by  $1/\rho$ . Indeed,  $\Phi(t)$  yields almost a straight line for  $t\Omega > 2$ , but the slope is not the one expected from the true long-time behaviour. The correction term  $C(t)$  is still too large to be negligible. On the other hand,  $C(t)$  varies so slowly that  $G(t)$  practically yields a straight line also, where however the slope is renormalised to  $1/\rho(1 + C)^{1/2}$ . The result (3.5) describes the solution well.

Let us now reconsider a normal transition point slightly away from the endpoint, but still on the critical surface  $S_c$ , characterised by  $\lambda < 1$ . For this case equation (3.4a) is to be replaced by equation (3.6a) of GS:

$$G_a(t) = (t_0/t)^a. \tag{3.7a}$$

For small  $1 - \lambda$  the small positive exponent  $a$  is related to the exponent parameter  $\lambda$  by equation (3.7a) of GS:

$$1 - \lambda = \zeta(2)a^2. \tag{3.7b}$$

This result describes the decay for  $t$  exceeding some crossover time  $t_0^c$ , where  $t_0^c \rightarrow \infty$  for

$a \rightarrow 0$ . We shall now show that the relaxation within the window  $t_m \ll t \ll t_0^c$  is described by the endpoint relaxation formula (3.4) or (3.5). The result will be found by studying the stability of the solution for  $\lambda = 1$  at points on the transition hypersurface  $S_c$ . These points are defined by  $\delta_0^c = \delta_1^c = 0$ , and being near to the endpoint implies  $\delta_2 \sim a^2$  to be small. Equation (2.4) then simplifies to

$$\text{LT}[G^2(t)](z) + zG^2(z) - \zeta(2)a^2\text{LT}[G^2(t)](z) - \mu\text{LT}[G^3(t)](z) + \dots = 0. \tag{3.8}$$

It is left to the reader to check that those terms neglected in the dynamic equation do not influence the leading-order critical correlations. As above we write the correlator as function of  $\ln t$ , equation (3.3), and use equations (A.4), (A.5) and (A.7) of the Appendix to derive in leading order the differential equation  $\zeta(2)(g'^2 - a^2g^2) = \mu g^3$ . Hence one gets

$$G(t) = \rho^2 a^2 p(ya) \tag{3.9a}$$

$$y = \ln(t/t_1). \tag{3.9b}$$

Here function  $p$  is independent of parameter  $a$ . It is a solution of the equation  $p' = -(p^2 + 4p^3)^{1/2}$ . Hence

$$p(y) = \frac{1}{4}[\coth^2(y/2) - 1] \tag{3.9c}$$

where the integration constant is absorbed in  $t_1$ . Equivalently, one can represent the result also as

$$G(t) = \rho^2 a^2 q((t/t_1)^a) \tag{3.10}$$

where  $q(x) = p(\ln x)$ . For small  $y$  one gets  $p(y \ll 1) = 1/y^2$  and this reproduces equation (3.4a) for the critical spectrum. For large  $y$  one finds  $p(y \gg 1) = \exp(-y)$  and this reproduces the power law, equation (3.7a). The critical correlator found depends sensitively on two variables: the time entering as  $\ln(t/t_1)$ , and the small number  $a$ , specifying the separation from the endpoint. The result is given by a scaling law. Changes of  $a$  are equivalent to changes of scale. The scale of the correlator  $\rho^2 a^2$  decreases for  $\lambda \rightarrow 1$ . The scale of  $\ln(t/t_1)$  increases like  $1/a$  upon approaching the endpoint. The rescaled correlator  $G/a^2$ , considered as a function of the rescaled variable  $\ln(t/t_1)a$ , is given by an  $a$ -independent master function  $p$ . The scaling law describes a crossover phenomenon. For small values of  $a \ln(t/t_1)$  one finds the logarithmic decay law  $G_0$  characteristic for the endpoint, equation (3.4a); while the true long-time asymptotics is given by a power-law correlator  $G_a$ , equation (3.7a). The crossover occurs for  $ya \approx 2$ , i.e. for

$$t_0^c = t_1 \exp(2/a) = t_1 \exp\{2[\zeta(2)/(1 - \lambda)]^{1/2}\}. \tag{3.11}$$

At the crossover the correlator has the small value  $G(t_0^c) \approx (1 - \lambda)/\mu$ . Similar crossovers occur in the critical spectra. For small frequencies the true asymptotic sublinear variation of the susceptibility is obtained, which is characteristic for a normal type B transition (Götze and Sjögren 1989):

$$\chi''(\omega) = (\omega t_0)^a \sin(\pi a/2)\Gamma(1 - a) \quad \omega t_0^c \ll 1. \tag{3.12a}$$

Approaching the endpoint, the range of validity of this result shrinks to zero. Outside this frequency range the endpoint critical spectrum is derived from equations (3.9c) or (3.4b):

$$\chi''(\omega) \approx \pi \rho^2 / \{\ln[1/(\omega t_1)]\}^3 \quad \omega t_0^c \gg 1. \tag{3.12b}$$

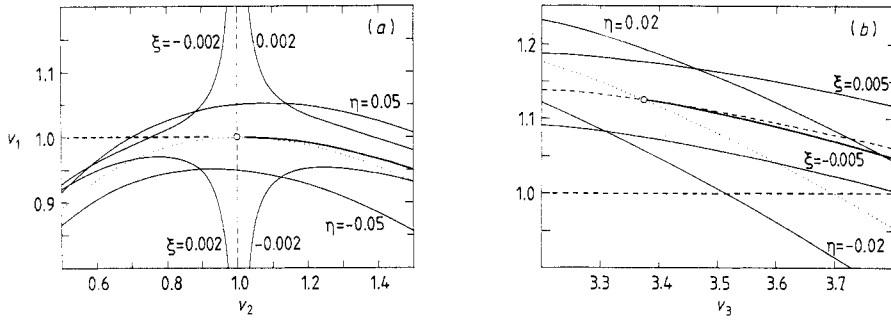


**Figure 2.** (a) Coordinate system  $(\xi, \eta)$  for the  $F_{12}$  model close to the endpoint  $v_1 = v_2 = 1$ . The full and broken heavy curves show the transition line for the B and A transitions respectively. Light full curves indicate constant  $\xi$  and  $\eta$  surfaces. The dotted curve shows the surface  $\eta = 0$ , and the light broken curve the surface  $\xi = 0$ . (b) Same as (a) but for the  $F_{13}$  model.

#### 4. $\beta$ relaxation near simple endpoints

In order to discuss the  $\beta$  relaxation near simple endpoints, but not necessarily on the critical surface  $S_c$ , it is useful to introduce natural coordinates. The system of coordinates  $(\sigma, \lambda)$ , the separation and exponent parameters used for the discussion of normal glass transitions in GS, is not well adopted for the present problem. For that coordinate system the  $\lambda = 1$  hypersurface defines a boundary and so only half of the neighbourhood of the endpoint can be described by it (see figures 1(a) and (b) in GS). Since  $\lambda = 1$  is the defining property of the endpoint, we will use this equation for all points near the endpoint  $V_c$ . So let us specify  $\tilde{f}$  such that

$$\delta_2[\tilde{f}(V), V] = 0 \quad \tilde{f}(V_c) = f_c. \quad (4.1a)$$

The condition  $\mu \neq 0$  is equivalent to  $\partial \delta_2 / \partial \tilde{f} \neq 0$  and therefore  $\tilde{f}(V)$  is defined uniquely as a smooth function of  $V$  for all  $V$  near  $V_c$ . Let us characterise the neighbourhood of the endpoint through the two parameters

$$\xi(V) = \delta_0[\tilde{f}(V), V] \quad (4.1b)$$

$$\eta(V) = \delta_1[\tilde{f}(V), V] \quad (4.1c)$$

which become zero at the endpoint. One can consider the transition from  $(v_1, v_2, \dots, v_N)$  to  $(\xi, \eta, v_3, \dots, v_N)$  as coordinate transformation in parameter space. The construction of the hypersurfaces  $\xi = \text{constant}$  or  $\eta = \text{constant}$  is as elementary as explained in GS. Figures 2(a) and (b) illustrate the result for the  $F_{12}$  and  $F_{13}$  models respectively. While figure 2(b) exhibits the generic case, figure 2(a) shows some peculiarities due to the coincidence of A-line and B-line endpoints.

Using the new coordinates, the equation of motion (2.4) takes the form

$$zG^2(z) + \text{LT}[G^2(t)](z) + (-\xi/z) + \eta G(z) - \mu \text{LT}[G^3(t)](z) + \dots = 0. \quad (4.2)$$

Here we have anticipated that the neglected terms do not contribute to the leading-order result for  $\xi \rightarrow 0$ ,  $\eta \rightarrow 0$ ,  $z \rightarrow 0$ . One has to check this after construction of the solution; a task which is left to the reader. One notices that only the two coordinates  $\xi, \eta$  are relevant for the discussion. For  $\mu$  we can take its value at  $V_c$ .



The new coordinate system overlaps the previously used one and it is of some interest to understand this in detail. So let us describe the variables  $\sigma$  and  $\lambda$  in terms of  $\xi$  and  $\eta$ . To proceed one introduces a renormalisation of  $\hat{f}$  by writing

$$G(t) = \delta f + F(t). \quad (4.3a)$$

Substitution into equation (4.2) yields

$$\begin{aligned} zF^2(z) + \Lambda_{\text{LT}}[F^2(t)](z) \\ + (-\Delta_0/z) + \Delta_1 F(z) - \mu_{\text{LT}}[F^3(t)](z) = 0 \end{aligned} \quad (4.3b)$$

where the following abbreviations are used:

$$\Lambda = 1 - 3\mu\delta f \quad \Delta_0 = \xi + \eta\delta f - \mu\delta f^3 \quad \Delta_1 = \eta - 3\mu\delta f^2. \quad (4.3c)$$

The old coordinates have been defined by using such  $\delta f$  that  $\Delta_1 = 0$ ,  $\Lambda = \lambda < 1$ . Hence  $\delta f = (\eta/3\mu)^{1/2}$ . Since  $\sigma = \Delta_0$ , the chosen  $\delta f$  implies

$$1 - \lambda = 3\mu(\eta/3\mu)^{1/2} \quad \sigma = \xi + \frac{2}{3}\eta(\eta/3\mu)^{1/2}. \quad (4.4)$$

So the part of parameter space  $\eta > 0$  was covered by the discussion of GS. The boundary  $\lambda = 1$  is the hypersurface  $\eta = 0$ . The corresponding curves are shown dotted in figures 2(a) and (b). The hypersurface  $S_c$  of normal transition points is characterised by  $\sigma = 0$ , i.e.

$$S_c: \quad \xi = -\frac{2}{3}\eta(\eta/3\mu)^{1/2} \quad \eta > 0. \quad (4.5)$$

For the  $F_{12}$  and  $F_{13}$  models the phase transition lines are shown in figures 2(a) and (b) as heavy curves. The endpoints  $\xi = \eta = 0$  are marked by small open circles.

For points so close to  $S_c$  that  $t_0^c \leq t_\sigma = t_0/|\sigma|^{1/2a}$ , the dynamics can be understood from the result of § 3, and from the general results for the dynamics of normal transitions. Here  $t_0^c$  and  $a$  are given by equations (3.11) and (3.7b), (4.4). For times between  $t_m$  and  $t_0^c$  one finds the critical endpoint dynamics, given by equations (3.4). For larger times the  $\beta$  relaxation of  $A_2$  singularities describes the decay. So for  $t_0^c < t < t_\sigma$  the critical power law, equation (3.7a), is observed. For  $\sigma > 0$  and  $t > t_\sigma$ ,  $G(t)$  approaches exponentially its asymptotic value, given by the glass form factor. For  $\sigma < 0$  and  $t_\sigma < t < \tau$ ,  $G(t)$  continues to decay as described by the von Schweidler law, equations (4.18) in GS. The time  $\tau$  is the scale for the  $\alpha$  process. The dynamics for  $t > \tau$  is outside the range of validity of the present equations. The susceptibility spectrum exhibits the known  $\alpha$  peak located at  $\omega \sim 1/\tau$ .

The critical correlations are stable against the two perturbations proportional to  $\xi$  and  $\eta$  in equation (4.2), if  $|\xi/\mu| \ll |z_{\text{LT}}[G_0^3(t)](z)|$  and  $|\eta G_0(z)/\mu| \ll |z_{\text{LT}}[G_0^3(t)](z)|$ , where  $\mu$  is of order unity. These inequalities define two timescales  $t_\xi$  and  $t_\eta$  or corresponding frequency scales  $\omega_\xi$  and  $\omega_\eta$ . Substituting equations (3.4) one finds

$$t_\xi = 1/\omega_\xi = t_1 \exp[\rho(\mu/|\xi|)^{1/6}] \quad (4.6a)$$

$$t_\eta = 1/\omega_\eta = t_1 \exp[\rho(\mu/|\eta|)^{1/4}] \quad (4.6b)$$

and

$$G(t < \text{Min}(t_\xi, t_\eta)) = G_0(t) \quad (4.7a)$$

$$G(|z| > \text{Max}(\omega_\xi, \omega_\eta)) = G_0(z). \quad (4.7b)$$

This result generalises the findings of the preceding section to arbitrary points near  $V_c$ .

For short times relative to the scales  $t_\xi, t_\eta$  the critical endpoint relaxation is observed. The interval for the validity of equations (4.7) expand exponentially if  $(\xi, \eta) \rightarrow (0, 0)$ . The critical correlator  $G_0(t)$  describes the decay down to the small value

$$G(t \propto \text{Min}(t_\xi, t_\eta)) = \text{Max}((|\xi|/\mu)^{1/3}, (|\eta|/\mu)^{1/2}). \tag{4.7c}$$

In order to go beyond the above critical region, let us express the correlator as function of  $\ln t$  as in equation (3.3). According to equations (A.2), (A.5) and (A.7) the dynamic equation (4.2) reduces in leading order to the differential equation  $\xi(2)g'^2 + \xi + \eta g - \mu g^3 = 0$ . We rewrite it into an explicit equation such that  $g'(y) < 0$  for large  $y$ :

$$g(y) = \rho^2 p(y) \tag{4.8}$$

$$p' = -(4p^3 - g_2 p - g_3)^{1/2}. \tag{4.9}$$

Here the following abbreviations are introduced:

$$g_2 = (4\eta/\mu)/\rho^4 \quad g_3 = (4\xi/\mu)/\rho^6. \tag{4.10}$$

The results (4.7) are rediscovered if  $g_2 p$  and  $g_3$  can be neglected in equation (4.9). So one gets

$$p(y) = 1/(y - y_1)^2 \quad y - y_1 \rightarrow +0. \tag{4.11}$$

Here the integration constant  $y_1 = \ln t_1$  fixes the microscopic timescale in equations (3.4). According to the discussions above one can use the asymptotic result (4.11) qualitatively up to  $y - y_1 \approx 1$ . One then gets

$$p(y - y_1 \approx 1) \approx 1. \tag{4.12}$$

In addition to  $S_c$  there are two further hypersurfaces exhibiting transparent relaxations which can be described by logarithmic scaling laws. On the hypersurfaces  $\lambda = 1$ , indicated by dotted lines in figures 2(a) and (b), one gets  $g_2 = 0$ . Let us for the moment restrict ourselves to  $\xi < 0$ . From equation (4.9) one finds:

$$G(t) = (|\xi|/\mu)^{1/3} p_1(y_\xi) \tag{4.13a}$$

$$y_\xi = \ln(t/t_1)/\ln(t_\xi/t_1). \tag{4.13b}$$

Here the master function obeys  $p' = -2(p^3 + 1)^{1/2}$ . The integration constant  $y_1$  in equation (4.11) has been eliminated by introducing  $t_1$ . So one gets  $p(y \rightarrow 0) = 1/y^2$ . For  $p \rightarrow 0$  one finds  $p \rightarrow -2(y + y_0)$ . The result has to be compatible with equation (4.12) and this requires  $y_0 = -\frac{3}{2}C_1$ , where  $C_1$  is of order unity. So the scaling law (4.13) describes the crossover from the critical decay to a simple logarithmic time variation:

$$G(t) = (-2/\rho)(|\xi|/\mu)^{1/2} \ln(t/t'_\xi) \quad \eta = 0 \tag{4.14a}$$

where

$$t'_\xi/t_1 = (t_\xi/t_1)^{3C_1/2}. \tag{4.14b}$$

This law is valid for  $t_\xi \ll t \ll t''_\xi$ , where the new scale

$$t''_\xi = t'_\xi \exp[\rho(\mu/|\xi|)^{1/2}] \tag{4.14c}$$

is the relevant one for the  $\alpha$  process. These formulae extend a recent result (Götze and Haussmann 1988) in two respects. First, the previously unspecified scale  $t'_\xi$  is now

determined. Secondly, the time interval for the validity of equation (4.14a) is understood and the relevant range in parameter space is identified as the neighbourhood of the  $\lambda = 1$  or  $\eta = 0$  hypersurface.

The hypersurfaces  $\xi = 0, \eta < 0$  are located in the centre of that region which is not covered by the  $\lambda$ - $\sigma$  coordinate system, as seen from equation (4.4). The respective lines are shown in figures 2(a) and (b) as light broken lines. From equation (4.10) one gets the characterisation for these parameter points:  $g_3 = 0, g_2 < 0$ . Equations (4.6), (4.8) and (4.9) imply again a logarithmic scaling law

$$G(t) = (|\eta|/\mu)^{1/2} p_{II}(y_\eta) \tag{4.15a}$$

$$y_\eta = \ln(t/t_1)/\ln(t_\eta/t_1). \tag{4.15b}$$

In this case the master function follows from the differential equation  $p' = -2(p^3 + p)^{1/2}$ . The large  $p$  behaviour is the same as above. In the opposite limit one finds  $p \rightarrow (y_0 - y)^2$  for  $y < y_0$ . The correct matching according to equation (4.12) requires  $y_0 = 2C_{II}$ , where  $C_{II}$  is of order unity. So the result describes a crossover from the critical decay to a quadratic logarithmic variation

$$G(t) = (|\eta|/\mu\rho^2) \ln^2(t'_\eta/t) \quad \xi = 0 \tag{4.16a}$$

$$t'_\eta = t_1(t_\eta/t_1)^{2C_{II}}. \tag{4.16b}$$

This law holds for  $t_\eta \ll t \ll t'_\eta$ , where the latter time again is the scale for the  $\alpha$  decay.

The dynamics near  $A_2$  singularities is governed by one scale  $t_\sigma$ . Approaching the normal glass transition,  $\sigma \rightarrow 0$ , this time diverges. This divergence is a manifestation of the slowing down of the dynamics near the critical points. The dynamics near the  $A_3$  singularity is ruled by the two timescales  $t_\xi, t_\eta$ . Again their divergence near the endpoint characterises the slowing down of the dynamics. The decay laws (4.14a) and (4.16a) are the analogues of the von Schweidler law. This latter law describes the high-frequency tail of the  $\alpha$  peak in the susceptibility spectrum. The present results do not describe such a peak. In leading low-frequency expansion equation (A.2) yields for the correlators

$$G(z) = (1/z)(2/\rho)(|\xi|/\mu)^{1/2} \ln(1/-izt'_\xi) \quad t''_\xi^{-1} \ll |z| \ll t_\xi^{-1} \quad \eta = 0 \tag{4.17a}$$

$$G(z) = -(1/z)(|\eta|/\mu\rho^2) \ln^2(1/-izt'_\eta) \quad t''_\eta^{-1} \ll |z| \ll t_\eta^{-1} \quad \xi = 0. \tag{4.17b}$$

Therefore the asymptotic form of the susceptibility spectra  $\chi''(\omega) = \omega G''(\omega)$  reads

$$\chi''(\omega) = \pi(|\xi|/\mu\rho^2)^{1/2} \quad t''_\xi^{-1} \ll \omega \ll t_\xi^{-1} \quad \eta = 0 \tag{4.18a}$$

$$\chi''(\omega) = -\pi(|\eta|/\mu\rho^2) \ln(1/\omega t'_\eta) \quad t''_\eta^{-1} \ll \omega \ll t_\eta^{-1} \quad \xi = 0. \tag{4.18b}$$

Let us finally consider the cases when  $\xi > 0$  and  $\eta > 0$ . From equation (4.3) it is evident that in this case we can find a solution where  $G(t)$  tends to a constant  $\delta f$  for  $t \rightarrow \infty$ . Introducing  $\delta f = \rho^2 f_0$  we have

$$4f_0^3 - g_2 f_0 - g_3 = 0. \tag{4.19}$$

Along the hypersurfaces  $\eta = 0$  and  $\xi = 0$  this equation is solved simply. For  $g_2 = 0$  we find  $f_0 = (\xi/\mu)^{1/3} \rho^{-2}$  and for  $g_3 = 0$  we find  $f_0 = (\eta/\mu)^{1/2} \rho^{-2}$ . These constants match the critical decay for  $t = t_\xi$  and  $t = t_\eta$  respectively as is seen from equation (4.7c). So for  $\xi > 0, \eta > 0$  we find a critical decay whereafter there is a crossover to a constant value.

The results above have been tested by numerical solution of equation (2.1) for the  $F_{12}$  model close to its endpoint  $v_1 = v_2 = 1$ . The results along the two hypersurfaces  $\eta =$

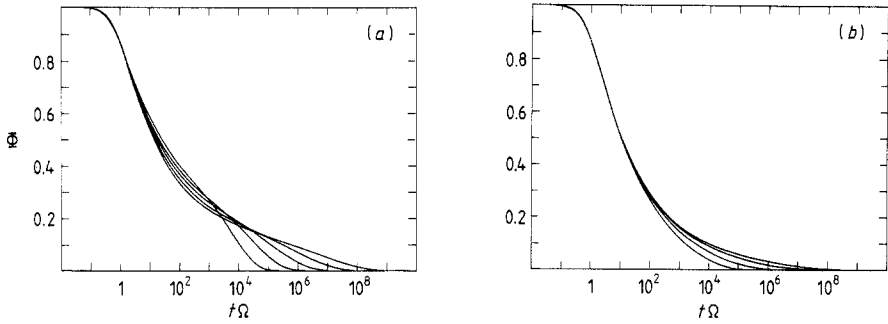


**Figure 3.** (a) Plot of  $\Phi(t)$  versus  $t\Omega$  for the  $F_{12}$  model. The various curves correspond to  $\nu = 5\Omega$ ,  $\eta = 0$ , and at long times from left to right  $\xi = -0.008/2^n$  ( $n = 0-4$ ). (b) Plot of  $\Phi(t)$  as in (a) but for parameters  $\xi = 0$ , and from left to right  $\eta = -0.05/2^n$  ( $n = 0-3$ ).

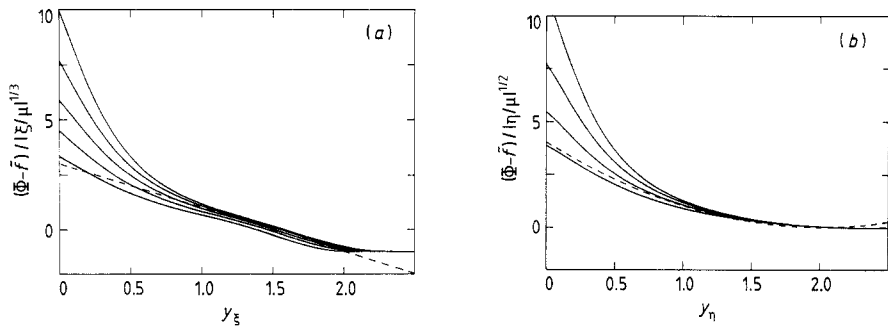


**Figure 4.** (a) Plot of  $\{\Phi[t_1(t_\xi/t_1)^{y_\xi}] - \tilde{f}\} / |\xi/\mu|^{1/3}$  versus  $y_\xi$  and with  $t_1\Omega = 1$ . The various curves correspond to those in figure 3(a). The broken line shows the straight line  $-2(y_\xi - \frac{3}{2})$ . (b) Plot of  $\{\Phi[t_1(t_\eta/t_1)^{y_\eta}] - \tilde{f}\} / |\eta/\mu|^{1/2}$  versus  $y_\eta$  and with  $t_1\Omega = 1$ . The various curves correspond to those in figure 3(b). The broken curve shows the parabola  $(y_\eta - 2)^2$ .

0 and  $\xi = 0$  are shown in figures 3(a) and (b) respectively. The results refer to  $\nu = 5\Omega$  and the parameter values  $\xi = -0.008/2^n$  ( $n = 0-4$ ) and  $\eta = -0.05/2^n$  ( $n = 0-3$ ). After an initial microscopic decay for  $t \leq 1/\Omega$  we see the critical decay law. In figure 3(a) this is followed by a clear crossover to a  $\ln(t/t'_\xi)$  decay according to equation (4.14a), while in figure 3(b) the crossover to the predicted  $\ln^2(t/t'_\eta)$  decay in equation (4.16a) is smoother. The data in figure 3 have also been rescaled according to (4.13) and (4.15) in order to test the scaling behaviour. The results are shown in figures 4(a) and (b) respectively. It is seen that for small rescaled times there are large deviations from scaling but for longer rescaled times all curves fall essentially on one master curve. The broken curves in figures 4(a) and (b) denote the straight line  $-2(y_\xi - \frac{3}{2})$  and the parabola  $(y_\eta - 2)^2$  respectively. The large deviations from the critical decay law are further illustrated in figure 5 where we show  $[\Phi(t) - \tilde{f}]^{-1/2}$  for the curves in figure 3 corresponding to  $\xi = -0.0005$  and  $\eta = -0.00625$  respectively. The broken curve is the asymptotic law  $G_0(t)$  in equation (3.4a) and the dotted curve is  $G(t)$  from equation (3.5a). In order to see fully the critical decay one has to go to even smaller  $\xi$  and  $\eta$  values. The susceptibility spectra corresponding to the data in figure 3 are shown in figure 6. Figure 6(a) clearly shows the development of the plateau value in equation (4.18a) and in figure 6(b) there is some indication of a crossover from a critical decay for  $10^{-4} < \omega/\Omega < 10^{-2}$  to a linear decay for smaller  $\omega$  as predicted by equation (4.18b).

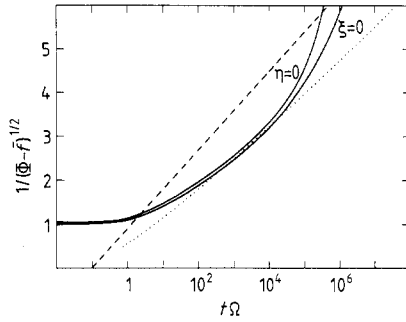


**Figure 5.** Plot of  $[\Phi(t) - \tilde{f}]^{-1/2}$  versus  $t\Omega$  for the curves in figure 3 corresponding to  $\xi = -0.0005$  and  $\eta = -0.00625$ . The broken curve represents the result  $G_0(t)$  in (3.4a) and the dotted curve the result in equation (3.5a), both with  $t_1\Omega = 0.1$ .

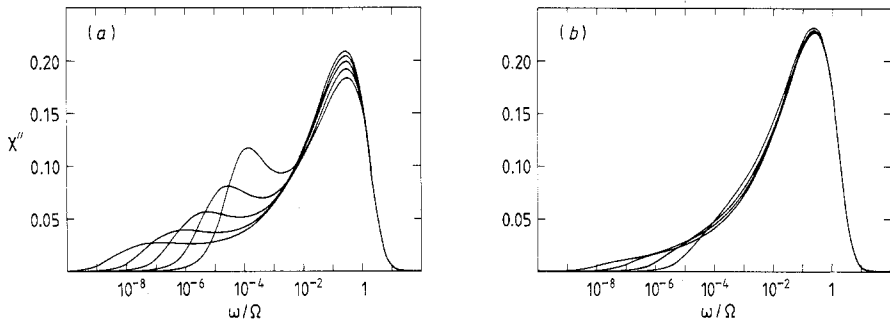


**Figure 6.** (a) Plot of  $\chi''(\omega)$  versus  $\omega/\Omega$  for the data shown in figure 3(a). (b) Plot of  $\chi''(\omega)$  versus  $\omega/\Omega$  for the data shown in figure 3(b).

The preceding analysis brought out simple relaxation laws if the parameters are chosen on certain hypersurfaces. By continuity the results describe the relaxation also for parameters near the specified sets:  $\sigma = 0$ ,  $\eta = 0$  or  $\xi = 0$ . There now appear a large variety of crossover phenomena if one moves in parameter space from one hypersurface to another. They are described by the general solution of equation (4.9) with initial condition (4.11). This is the Weierstrass elliptic function with invariants  $g_2$  and  $g_3$  (Gradshteyn and Ryzhik 1965, ch 8.16).

$$G(t) = \rho^2 \mathcal{P}[\ln(t/t_1); g_2, g_3]. \tag{4.20}$$

This function exhibits the homogeneity property

$$\mathcal{P}(y; g_2, g_3) = s^2 \mathcal{P}(sy; s^{-4}g_2, s^{-6}g_3) \tag{4.21}$$

which can be read off from equation (4.9) easily. Applying this formula for  $s = 1/\ln(t/t_1)$ , expressing the parameters in terms of the scales, equations (4.6) and (4.10), and using the notations (4.13b) and (4.15b) one can write the result for the  $\beta$  dynamics in the whole neighbourhood of the endpoint in the condensed form:

$$G(t) = [\rho/\ln(t/t_1)]^2 p(y_\eta, y_\xi) \tag{4.22a}$$

$$p(y_\eta, y_\xi) = \mathcal{P}(1; \pm 4y_\eta^4, \pm 4y_\xi^6). \tag{4.22b}$$

The sign alternatives refer to  $\eta \geq 0$  and  $\xi \geq 0$  respectively. This formula expresses  $G(t)$  as a two-parameter logarithmic scaling law.

The Laurent series of  $\mathcal{P}$  yields the critical correlator as leading contribution and power series expansion in terms of  $y_\eta^4$  and  $y_\xi^6$  for the corrections:

$$G(t) = G_0(t)(1 \pm \frac{1}{5}y_\eta^4 \pm \frac{1}{7}y_\xi^6 + \dots). \tag{4.23}$$

This formula covers the whole neighbourhood of the endpoint including the transition hypersurface  $S_c$ . The expected power laws, equation (3.7a), are here expanded for small exponent  $a$ :  $(t_0/t)^a = 1 + a \ln(t_0/t)$ .

Applying the homogeneity equation (4.21) yields

$$\mathcal{P}(1; \pm 4y_\eta^4, \pm 4y_\xi^6) = s^2\mathcal{P}[s; \pm 4(y_\eta/s)^4, \pm 4(y_\xi/s)^6]. \tag{4.24}$$

Choosing  $s = y_\xi$  or  $s = y_\eta$  one can rewrite the two-parameter logarithmic scaling law in the equivalent forms

$$G(t) = (|\xi|/\mu)^{1/3} \mathcal{P}[y_\xi; \pm 4(y_\eta/y_\xi)^4, \pm 4] \tag{4.25a}$$

$$G(t) = (|\eta|/\mu)^{1/2} \mathcal{P}[y_\eta; \pm 4, \pm 4(y_\xi/y_\eta)^6]. \tag{4.25b}$$

Comparison with equations (4.13a) and (4.15a) thus yields the formulae for the master functions in terms of  $\mathcal{P}$ :

$$p_I(y) = \mathcal{P}(y; 0, -4) \tag{4.26a}$$

$$p_{II}(y) = \mathcal{P}(y; -4, 0). \tag{4.26b}$$

Expanding equations (4.25) with respect to  $g_2$  or  $g_3$  yields the leading corrections to the scaling laws (4.13a) or (4.15a):

$$G(t) = (|\xi|/\mu)^{1/3} p_I(y_\xi)[1 + f_I(y_\xi)(y_\eta/y_\xi)^4 + \dots] \tag{4.27a}$$

$$G(t) = (|\eta|/\mu)^{1/2} p_{II}(y_\eta)[1 + f_{II}(y_\eta)(y_\xi/y_\eta)^6 + \dots]. \tag{4.27b}$$

For the prefactors of the corrections one finds

$$f_I = \frac{1}{3}[\frac{1}{2}(\mathcal{P}'/\mathcal{P})\zeta + \mathcal{P}] \tag{4.28a}$$

$$f_{II} = -\frac{1}{4}[3(\mathcal{P}'/\mathcal{P})\zeta + 6\mathcal{P} + 4/\mathcal{P}]. \tag{4.28b}$$

Here  $\zeta$  denotes Weierstrass'  $\zeta$  function and the arguments are the same as in equations (4.26a) or (4.26b) respectively. These formulae quantify the corrections to the logarithmic decay laws (4.14a) and (4.16a) if one moves away from the specified hyperplanes  $\eta = 0$  or  $\xi = 0$  respectively.

For a discussion of the properties of  $\mathcal{P}$  the discriminant  $\Delta = g_2^3 - 27g_3^2$  is of importance. From equation (4.10) one finds

$$\Delta = (432/\rho^{12})[4(\eta/3\mu)^3 - (\xi/\mu)^2]. \tag{4.29a}$$

For the region of definition of the coordinates  $(\sigma, \lambda)$  one can write with equation (4.4)

$$\Delta = (432/\rho^{12}\mu^2)[\frac{2}{3}\eta(\eta/3\mu)^{1/2} - \xi]\sigma. \tag{4.29b}$$

Hence the transition hypersurface  $S_c$  is characterised by  $\Delta = 0$ . Near  $S_c$  one can simplify this expression to

$$\Delta = (64/\mu^4\rho^{12})(1 - \lambda)^3\sigma. \tag{4.29c}$$

Equation (4.9) can be written as  $\mathcal{P}' = -2[(\mathcal{P} - e_1)(\mathcal{P} - e_2)(\mathcal{P} - e_3)]^{1/2}$  where the roots

$e_k$  are the solutions of equation (4.19). Thus  $\Delta > 0$  characterises the region where there are three different solutions for  $f_0$ . At the phase transition hypersurface two roots are degenerate and at the simple endpoint all three roots coincide. The normal transition anomalies are obtained therefore by specialising equation (4.20) to small  $\Delta$ . The results are known from GS and will not be repeated.

## 5. Conclusions

The most general mode-coupling theories of the idealised glass transition studied so far deal with sets of correlators  $\Phi_q(t)$ , describing the relaxation of density or spin-density excitations of wavevector  $q$  (Bengtzelius *et al* 1984, Götze and Sjögren 1984). The equation of motion has the form (2.1), where however  $\nu, \Omega, F$  are to be generalised to wavevector-dependent quantities  $\nu_q, \Omega_q, F_q$ . The functions  $\nu_q, \Omega_q$  do not enter the scale-invariant equation for the correlators near glass transition singularities. The mode-coupling functional has the general form

$$F_q[\Phi_k(t)] = \sum_l (1/l!) \sum_{k_1 \dots k_l} V^{(l)}(q; k_1, \dots, k_l) \Phi_{k_1}(t) \dots \Phi_{k_l}(t). \quad (5.1)$$

The non-negative decay vertices  $V^{(l)}$  are the mathematical control parameters. They depend smoothly on the physical control parameters  $x_1, x_2, \dots, x_M$ , like temperature  $T$ , magnetic field  $B$ , density  $n$ , etc. The crucial new concept entering the discussion of  $\beta$  relaxation of systems described by more than one correlator is the stability matrix

$$C_{qk} = [\partial F_q(f_k)/\partial f_k]_c (1 - f_k^c)^2. \quad (5.2)$$

It is essentially the Jacobian matrix evaluated at the bifurcation points  $V_c$ . This matrix is a non-degenerate Frobenius matrix and thus it has a non-degenerate maximum eigenvalue  $E_0$ . The critical points are characterised by  $E_0 = 1$ . The left and right eigenvectors  $\hat{l}_q, l_q$  are uniquely determined by the normalisation requirements:

$$l_q > 0 \quad \hat{l}_q > 0 \quad \sum_q \hat{l}_q l_q = 1 \quad \sum_q \hat{l}_q (1 - f_q^c) l_q = 1. \quad (5.3)$$

Then one finds for the correlator within the  $\beta$  region

$$\Phi_q(t) = \tilde{f}_q + h_q G(t) + h'_q G^2(t) + \dots \quad (5.4a)$$

where

$$h_q = (1 - \tilde{f}_q)^2 l_q \quad \sum_q \hat{l}_q h'_q = 0. \quad (5.4b)$$

Function  $G(t)$  is independent of  $q$  and it obeys equation (2.4). The parameters  $\delta_k, \gamma_k$  in this equation can be expressed in terms of  $V^{(l)}, \tilde{f}$  and  $\hat{l}_q$  and thus they are smooth functions of  $x_1, \dots, x_M$ . In this manner the general problem is reduced to one dealing with a single correlator  $G(t)$  only. The proofs of the preceding results can be found elsewhere (Götze 1985, 1987).

Notice that the last term of equation (5.4a) yields a correction to scaling laws of a different type than the ones discussed in the preceding calculations. This correction is of higher order, however. It does not modify the result (3.5), nor does it enter the next

correction to equation (3.5) which we have not evaluated explicitly. It is of order  $1/y^4$ . So all models yield as critical correlator at a Whitney cusp for  $y \rightarrow \infty$ :

$$\Phi_q(t) - f_q^c = h_q \tilde{\rho}^2 / y^2 \quad y = \ln(t/t_1) \quad (5.5a)$$

$$\tilde{\rho}^2 = \rho^2 [1 + 4.384(\ln y)/y + C/y]. \quad (5.5b)$$

Only those terms which vanish faster than  $1/y^3$  get a more complicated  $q$  dependence. If one is not at the cusp but close to it, equations (5.5) hold for  $y$  up to some crossover value. In certain regions of parameter space, specified in § 4, the crossover leads to the simple law

$$\Phi_q(t) - \tilde{f}_q = h_q (-2/\rho) (|\xi|/\mu)^{1/2} \ln(t/t'_\xi) \quad (5.6a)$$

or to

$$\Phi_q(t) - \tilde{f}_q = h_q (|\eta|/\mu\rho^2) \ln^2(t'_\eta/t). \quad (5.6b)$$

Here the scales  $t'_\xi, t'_\eta$  are defined in equations (4.14b), (4.16b) and (4.6). The variables  $(\xi, \eta)$  are the relevant mathematical control parameters for the neighbourhood of the singularity. Let us assume that there are two physical control parameters  $(x_1, x_2)$ , so that the critical point is specified by  $x_1 = 0, x_2 = 0$ . Generically, there is a non-singular  $2 \times 2$  matrix  $A_{ik}$ , so that

$$\begin{pmatrix} \xi \\ \eta \end{pmatrix} = \begin{pmatrix} A_{11} & A_{12} \\ A_{21} & A_{22} \end{pmatrix} \begin{pmatrix} x_1 \\ x_2 \end{pmatrix}. \quad (5.7)$$

Suppose one has worked out a mode-coupling theory for a microscopic model. As a result of such work one gets expressions for the wavevector-dependent quantities  $f_q, h_q$ , for the two numbers  $\mu, C$  and for the four matrix elements  $A_{ij}$ . No other results would enter the dynamics of the  $\beta$  relaxation near the cusp. Obviously, our theory has many non-trivial implications, where the mentioned information does not enter at all, like e.g. the whole shape of the various spectra.

The mathematical methods of our theory are general enough to deal also with higher-order cusps. The leading-order result for the critical correlator near an  $A_l$  singularity for  $l \geq 3$  follows from equation (3.1), as

$$\Phi_q(t) - f_q^c = h_q \{2\pi^2 / [3(l-2)^2 (-\delta_i^c)]\}^{1/(l-2)} / y^{2/(l-2)}. \quad (5.8)$$

The leading and next-to-leading corrections are given by a factor of the form  $[1 + C_1(\ln y)/y + C_2/y]$ . As opposed to the result of equation (5.5b) the constant  $C_1$  depends on the details like  $\gamma_\xi^c$  in equation (2.4) if  $l > 3$ . Consider as a special case  $l = 4$ . The general solution can be expressed in terms of a three-parameter scaling law. There will be regions in parameter space where one finds the laws (5.6). There appears furthermore a region where the critical decay in (5.8) is followed by the  $1/\ln^2(t/t_1)$  law of the Whitney cusp. These results follow from a discussion similar to that in §§ 3 and 4.

Recently glass transitions have been discussed within a Pott's model by Kirkpatrick and Thirumalai (1988). They derived dynamic equations under the assumption of small non-ergodicity parameters  $f_c$  and found their theory to reduce to our  $F_{12}$  model. Small  $f_c$  implies parameters in the neighbourhood of the endpoint shown in figure 2(a). Therefore our result (4.20) presents the solution of the specified model and our figures 3–6 exemplify the features of the specified dynamics. More recently Fisher and Huse (1988a, b) have formulated a phenomenological scaling theory for spin glasses. They study low excitations of spin droplets, which are characterised by several fractal dimen-



sionalities. They find in particular correlation decay according to a law  $m(t) \propto 1/\ln^x(t)$ , with an exponent  $x$  for which they can motivate upper and lower bounds. This law is compatible with our critical decay law, if one identifies  $x = 2/(l - 2)$  for the cuspid  $A_l$ , equation (5.8). They describe crossover phenomena by normal scaling laws, a result that is too simple to fit into our scenario.

The mode-coupling theory derives the waiting time statistics for the motion of the system through the potential landscape, defined in the high-dimensional configuration space. This motion can be characterised by a local stochastic time  $\Theta_t$  (Sjögren 1989, Götze and Sjögren 1989). Thus the present paper can be summarised by the statement that near  $A_3$  singularities the distribution for the local time satisfies  $E[\Theta_t] = y = \ln(t/t_1)$ , where  $E[\dots]$  denotes an average. On certain sets in parameter space conventional scaling laws are obtained. They have been called logarithmic scaling laws since  $t$  is replaced by  $E[\Theta_t]$ . As usual they describe the crossover from one power law to some other. In general the dynamics is more subtle, however. Two relevant timescales enter and this leads to two-parameter scaling laws. This reflects the fact that generically an  $A_3$  cuspid can be characterised only in a two-dimensional parameter space (Arnold 1986).  $\ln t$  is a slowly varying function, and we want to emphasise two implications of this property which follow from previous discussions of dynamic scaling laws. First, there is a transient interval of 0.5–1 decade between the region of microscopic motion and that region where corrections to scaling can be neglected; see figure 1. Secondly, one has to study the correlators over at least 1–2 decades in order to test the typical crossover phenomena described by scaling laws; see figure 5. In our case the decades refer to  $\ln t$  and not to  $t$  itself. Thus the whole relaxation is stretched out much further than is familiar from conventional power-law decay. One has to detect relaxation over huge intervals if one wants to discover the underlying scaling laws. On the other hand, corrections to scaling are slowly varying functions as well. So occasionally they may just be treated as constants. So we predict a critical power law (5.5a) to hold over, say, five decades of time variation, provided  $y$  is not too small. The prefactor  $\bar{\rho}^2$ , however, would not be equal to the value  $\rho^2$ . Rather it would be larger, and accurate measurements should bring out that it varies logarithmically with increasing time, as shown in figure 1(b).

The experimental findings for the dynamics of structural glass transitions fit the scenario of  $A_2$  singularities rather than that of  $A_3$  ones, as was indicated in the introduction. However, one should notice that generically the cusp singularities are located within the glass and not at the border between liquid and glass. Figure 2(b) shows a representative case, while figure 2(a) exhibits an exception in this context. The simple schematic model introduced by Bosse and Krieger (1986) for a discussion of the glass transition in ionic melts exhibits  $A_3$  lines and also one  $A_4$  point. Furthermore it was argued recently (Bosse *et al* 1988) that the relevant parameters for the description of the Ca–K–NO<sub>3</sub> glass former are close to the  $A_4$  cuspid. So endpoint singularities might be relevant and in this case one expects two anomalies. First, for temperatures  $T$  below the critical temperature  $T_c$  of the  $A_2$  transition, slow logarithmic decay and crossovers between logarithmic and power-law decays should occur. Secondly, the timescale  $\tau$  for  $\alpha$  relaxation, in particular the scales ruling transport coefficients like viscosity, should exhibit Vogel–Fulcher like variations with control parameters according to e.g. equation (4.14c). If the temperature is varied the system moves on a path  $V(T)$  in parameter space. The projections  $\xi(T)$ ,  $\eta(T)$  on the two relevant variables are important. Suppose that one hits the singularity for  $T = T_0$ :  $\xi(T_0) = \eta(T_0) = 0$ . Then our theory predicts

$$\tau \propto \exp[C/|T - T_0|^x] \quad (5.9)$$

with  $x = \frac{1}{2}$ ,  $\frac{1}{4}$  or  $\frac{1}{6}$  depending on the sector of parameter space under study. In general a

path might come close to  $V_c$ , but it will not hit it precisely, so  $\tau$  does not diverge. Hopping processes, which are ignored in this paper, will eliminate the divergence for  $T = T_0$  in equation (5.9) in any case (Götze and Sjögren 1987, 1988). So one may expect that equation (5.9) holds for  $T_0 < T < T_c$ , but if  $T$  approaches  $T_0$  function  $\tau(T)$  will remain finite and cross over e.g. to an Arrhenius behaviour. Such a scenario has been discussed often in the literature with  $\tau$  described by the Vogel–Fulcher law. This is equation (5.9) with  $x = 1$ . Under the specified conditions the laws with  $x = 1$  and  $x \neq 1$  cannot be discriminated experimentally.

Let us now consider the relaxation data for the Cu:Mn spin glass quoted in the introduction. Neutron scattering and muon spin relaxation determined  $\Phi(t)$  for  $10^{-12} < t < 10^{-8}$  s. The data have been fitted by a power-law decay  $\Phi(t) - \tilde{f} = A/t^a$  (Heffner and MacLaughlin 1984). The fit exponent  $a$  was 0.25 for  $T/T_g = 1.10$ , 0.94, where the glass transition temperature  $T_g$  is about 27.5 K. For lower temperatures exponent  $a$  was found to be 0.50. A power-law decay with a temperature-dependent exponent was predicted earlier by Sompolinsky and Zippelius (1982). However, they found  $a = \frac{1}{2}$  for  $T \geq T_g$  and obtained an  $a$  which decreased with decreasing temperature for  $T < T_g$ . A similar result follows from our  $\beta$  relaxation theory of type A transitions (Götze and Sjögren 1989). Thus the found temperature variation of exponent  $a$ , with a minimum around  $T_g$ , contradicts the mentioned theoretical pictures. Indeed, it was demonstrated that an explanation of the neutron scattering data within a simple type A transition scenario is not possible; one can describe reasonably the high- and low-temperature data but not the ones for  $T \sim T_g$  (Götze and Sjögren 1984). A fit of the neutron scattering data is possible within the  $F_{13}$  model, where  $\nu$  and  $v_3$  are constants and  $v_1$  varies linearly with  $1/T$ . The data for  $t > 10^{-11}$  s can be described by keeping the microscopic timescale  $\Omega$  fixed. If one wants to account also for the data at the shortest time  $t \sim 3 \times 10^{-12}$  s, one has to assume  $\Omega$  to decrease with decreasing temperature (Götze and Hausmann 1988). Within our present notations this means that the time  $t_1$  for the matching of microscopic motion and  $\beta$  relaxation increases with decreasing  $T$ . Mezei (1983, 1986) argued that the spin dynamics for  $t \leq 10^{-11}$  s is governed by thermally activated cluster motion. Thus the dynamics on microscopic scales is complicated and depends strongly on  $T$ , but these complications are not related to the glass transition problem. We adopt this view and accept therefore some  $T$  dependence of  $t_1$ . It is somewhat surprising that a data analysis worked within the  $F_{13}$  model, since this model imposes three artifacts, for which there is no microscopic justification: the value of the form factor  $f_c = \frac{1}{3}$ , a special variation of  $f$  with  $v_1$ , and the value  $\frac{1}{2}$  for the cusp parameter, equation (2.6b). These artifacts make it impossible to extend the quoted fit to larger times. So the remaining challenge is the explanation of the relaxation data for times exceeding  $10^{-8}$  s.

In figure 7(a) relaxation data for  $T = 26$  K and  $T = 20$  K are reproduced. The full circles with error bars are neutron scattering results (Mezei and Murani 1979), the open circles are AC susceptibility data (Murani *et al* 1981), and the full squares are muon spin relaxation results (Uemura *et al* 1984). A power-law fit of the data would require a value of exponent  $a < 0.2$ , which indicates that the parameters are close to an endpoint singularity. We expect that such a small number cannot be reached by the perturbation expansion of  $a - \frac{1}{2}$  using  $(T_g - T)/T_g$  as small parameter as implied by the theory of Sompolinsky and Zippelius (1982).

In order to test the critical decay law (5.5a) one has to show that there is some form factor  $f$  such that  $1/[\Phi(t) - f]^{1/2}$  is a linear function of  $\log(t/t_1)$ . This test requires the introduction of only one fit parameter  $f$ . Figure 7(b) shows such an analysis for the data

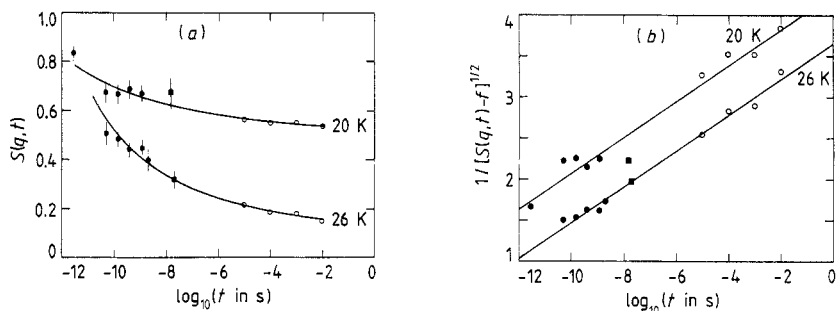


**Figure 7.** (a) Spin-density correlation function  $S(q, t)$  versus  $t$  for Cu:Mn. The full circles are the neutron scattering data of Mezei and Murani (1979), the open circles are the AC susceptibility measurements of Tholence (Murani *et al* 1981, Mezei 1983) and the full squares are the muon spin relaxation results of Uemura *et al* (1984). The full curves show the function  $f + A/\log^2(t/t_1)$ , where the parameters are taken from (b). (b) Plot of  $[S(q, t) - f]^{-1/2}$  for the experimental data in (a). For  $T = 26$  K we use  $f = 0.06$ , and for  $T = 20$  K,  $f = 0.47$ . The straight lines are the best fit to the experimental points and give for 26 K,  $y = 3.66 + 0.22 \log_{10}(t)$ , and for 20 K,  $y = 4.26 + 0.22 \log_{10}(t)$ ;  $t$  is in seconds.

of figure 7(a). For parameter values close to an endpoint, the regular variation of the prefactor as a function of  $T$  in equation (5.5a) should be negligible. Thus one expects the slopes in the plot to be the same for  $T = 26$  K and 20 K, as obtained by the fit. The scale  $t_1$  varies, as expected. Data analysis as done in figure 7(b) exaggerates data fluctuations if  $(\Phi - f)$  is small. So the elementary expression (5.5a), with parameters as chosen in figure 7(b) are also included as full curves in figure 7(a). Apparently, our theoretical results describe the experimental ones for a time interval extending over more than eight decades. Obviously, it would be very helpful to obtain more and better experimental data for the specified spin glass. One could try to extend the fit to even larger times. However, our theory ignores transport processes, which restore ergodicity for long times. They are described by the  $\alpha$  relaxation theory (Götze and Sjögren 1987, 1988). Therefore discrepancies between theory and experiment for long times might be caused by effects that are not of relevance in connection with our  $\beta$  relaxation theory. For these reasons it would be more informative to concentrate the work on the mesoscopic time interval of some decades above  $10^{-11}$  s. The following problems could be studied. It should be decided whether equation (5.5a) or rather equation (5.8) with  $l \geq 4$  describes the critical decay. We have tested the possibility of a critical decay law with  $l = 4$  and found a fit not much worse than the one shown in figure 7(b). So at present we cannot rule out the underlying singularity to be of higher order than the Whitney cusp. Data for  $28 \text{ K} < T < 30 \text{ K}$  could be used to study the predicted crossover phenomena from the critical to the simple logarithmic decay in equation (5.6a), and possibly even the general scaling laws. It would also be interesting to see whether crossover phenomena and the prefactor in equation (5.6a) depend sensitively on the magnetic field.

### Acknowledgments

We thank Professor A Sjölander for helpful discussions. WG thanks Nordita and Chalmers University for financial support and his colleagues in Göteborg for their kind hospitality. LS thanks the Swedish Natural Science Research Council for financial support.

**Appendix**

In this appendix we will outline a systematic method for solving the dynamic equations for  $\beta$  relaxation near endpoints. Let us start by reformulating the Laplace transforms of products of slowly varying functions. If one writes  $G(t) = g[\ln(t/t_1)]$  one gets

$$(-z)\text{LT}[G(t)](z) = \int_0^\infty du e^{-u} g(\ln u + y) \tag{A.1}$$

where  $y = \ln[1/(-izt_1)]$ . Taylor expansion of  $g$  around  $y$  yields

$$(-z)\text{LT}[G(t)](z) = g(y) + \Gamma_1 g'(y) + \frac{1}{2}\Gamma_2 g''(y) + \frac{1}{6}\Gamma_3 g'''(y) + \dots \tag{A.2}$$

Here

$$\Gamma_n = \int_0^\infty du e^{-u} \ln^n u \tag{A.3}$$

denotes the  $n$ th derivative of the gamma function at unity. The  $\Gamma_n$  can be expressed in terms of Euler's constant  $\gamma = 0.5772$  and Riemann's  $\zeta$  function (Gradshteyn and Ryzhik 1965, section 8.321). Replacing  $G$  by  $G^2$ ,  $G^3$  or  $G_1 G_2$  one finds

$$(-z)\text{LT}[G^2(t)](z) = g^2 + 2\Gamma_1 g g' + \Gamma_2 (g g'' + g'^2) + \frac{1}{3}\Gamma_3 (g g''' + 3g' g'') + \dots \tag{A.4}$$

$$(-z)\text{LT}[G^3(t)](z) = g^3 + 3\Gamma_1 g^2 g' + \frac{1}{2}\Gamma_2 (3g^2 g'' + 6g g'^2) + \dots \tag{A.5}$$

$$\begin{aligned} (-z)\text{LT}[G_1(t)G_2(t)](z) &= g_1 g_2 + \Gamma_1 (g'_1 g_2 + g_1 g'_2) \\ &+ \frac{1}{2}\Gamma_2 (g''_1 g_2 + 2g'_1 g'_2 + g_1 g''_2) + \dots \end{aligned} \tag{A.6}$$

For simplicity of notation the argument  $y$  is dropped in these and some of the following formulae. Combining the results one arrives at

$$(-z)\{\text{LT}[G^2(t)](z) + zG^2(z)\} = \zeta(2)g'^2 - 2[\gamma\zeta(2) + \zeta(3)]g'g'' + \dots \tag{A.7}$$

$$(-z)\{\text{LT}[G^3(t)](z) - z^2G^3(z)\} = 3\zeta(2)gg'^2 + \dots \tag{A.8}$$

$$(-z)\{\text{LT}[G_1(t)G_2(t)](z) - zG_1(z)G_2(z)\} = \zeta(2)g'_1 g'_2 + \dots \tag{A.9}$$

Notice that in these equations not only the leading terms cancel, as expected from the Tauberian theorem, but also the next-to-leading ones.

With equations (A.7) and (A.8), equation (3.1) for the critical correlator reduces in leading order to  $\zeta(2)g'^2 = \mu g^3$ . From the two alternatives  $g' = \pm (\mu/\zeta(2))^{1/2} g^{3/2}$  we choose the negative sign, since we are interested in a correlator which decreases for short times. Let us mention that the other alternative yields a solution of our equations which increases for short times. This solution of equation (3.1) has no relevance, since it violates the inequality (2.3b). Hence one gets

$$g_0(y) = [4\zeta(2)/\mu]/(y + y_0)^2 \tag{A.10}$$

where  $y_0$  denotes some integration constant. To find the dominant correction  $\delta g$ , we

substitute  $g = g_0 + \delta g$  into equation (3.1) and expand in linear order in  $\delta g$ . With the aid of equations (A.5) and (A.7)–(A.10) one finds the differential equation

$$y^4 \delta g' + 3y^3 \delta g = 24\zeta(3)/\mu. \quad (\text{A.11})$$

The general solution reads

$$\delta g = [24\zeta(3)/\mu] \ln y/y^3 + C/y^3. \quad (\text{A.12})$$

The integration constant  $C$  can be eliminated by a shift  $y_0 \rightarrow y_1$  in equation (A.10). Without alteration of the leading and next-to-leading terms, one can change in equation (A.12)  $y \rightarrow y + y_1$ . As a result one gets

$$g(y) = [4\zeta(2)/\mu]/(y + y_1)^2 + [24\zeta(3)/\mu] \ln(y + y_1)/(y + y_1)^3 + \dots \quad (\text{A.13})$$

Substitution of  $y + y_1 = \ln(t/t_1)$  then yields the desired result (3.4a) for the critical decay. After specification of  $g(y)$  in equation (A.13) one can check that the expansion in equation (A.2) and so forth are asymptotically correct.

## References

- Arnold V I 1986 *Catastrophe Theory* 2nd edn (Berlin: Springer)
- Bengtzelius U, Götze W and Sjölander A 1984 *J. Phys. C: Solid State Phys.* **17** 5915
- Binder K and Young A P 1986 *Rev. Mod. Phys.* **58** 801
- Bosse J and Krieger U 1986 *J. Phys. C: Solid State Phys.* **19** L609
- Bosse J, Krieger U and Thakur J S 1988 *Preprint*
- Feller W 1971 *An Introduction to Probability Theory and its Applications* 2nd Edn, vol. II (New York: Wiley)
- Fisher D S and Huse D A 1988a *Phys. Rev. B* **38** 373
- 1988b *Phys. Rev. B* **38** 386
- Götze W 1985 *Z. Phys. B* **60** 195
- 1987 *Amorphous and Liquid Materials* ed. E Lüscher, G Fritsch and G Jaccuci (Dordrecht: Martinus Nijhoff)
- Götze W and Haussmann R 1988 *Z. Phys. B* **72** 403
- Götze W and Sjögren L 1984 *J. Phys. C: Solid State Phys.* **17** 5759
- 1987 *Z. Phys. B* **65** 415
- 1988 *J. Phys. C: Solid State Phys.* **21** 3407
- 1989 *J. Phys. C: Solid State Phys.* **22** 4173
- Gradshteyn I S and Ryzhik I M 1965 *Tables of Integrals, Series and Products* (New York: Academic)
- Heffner R H and MacLaughlin D E 1984 *Phys. Rev. B* **29** 6048
- Kirkpatrick T R and Thirumalai D 1988 *Phys. Rev. B* **37** 5342
- Mezei F 1983 *J. Magn. Magn. Mater.* **31** 1327
- 1986 *Europhys. News* **17** 129
- Mezei F, Knaak W and Farago B 1987 *Phys. Rev. Lett.* **58** 571
- Mezei F and Murani A P 1979 *J. Magn. Magn. Mater.* **14** 211
- Murani A P, Mezei F and Tholence J L 1981 *Physica B* **108** 1384
- Richter D, Frick B and Farago B 1988 *Phys. Rev. Lett.* **61** 2465
- Sjögren L 1989 *Z. Phys. B* **74** 353
- Sompolinsky H and Zippelius A 1982 *Phys. Rev. B* **25** 6860
- Uemura Y J, Harshman D R, Senba M, Ansaldo E J and Murani A P 1984 *Phys. Rev. B* **30** 1606